Published OnlineFirst April 14, 2015; DOI: 10.1158/1078-0432.CCR-14-2751

Personalized Medicine and Imaging

Clinical Cancer Research

Superiority of [^{68}Ga]-DOTATATE PET/CT to Other Functional Imaging Modalities in the Localization of *SDHB*-Associated Metastatic Pheochromocytoma and Paraganglioma

Ingo Janssen[1,2], Elise M. Blanchet[3], Karen Adams[1], Clara C. Chen[4], Corina M. Millo[5], Peter Herscovitch[5], David Taieb[6], Electron Kebebew[7], Hendrik Lehnert[8], Antonio T. Fojo[9], and Karel Pacak[1]

Abstract

Purpose: Patients with succinate dehydrogenase subunit *B* (*SDHB*) mutation–related pheochromocytoma/paraganglioma (PHEO/PGL) are at a higher risk for metastatic disease than other hereditary PHEOs/PGLs. Current therapeutic approaches are limited, but the best outcomes are based on the early and proper detection of as many lesions as possible. Because PHEOs/PGLs overexpress somatostatin receptor 2 (SSTR2), the goal of our study was to assess the clinical utility of [^{68}Ga]-DOTA(0)-Tyr(3)-octreotate ([^{68}Ga]-DOTATATE) positron emission tomography/computed tomography (PET/CT) and to evaluate its diagnostic utility in comparison with the currently recommended functional imaging modalities [^{18}F]-fluorodopamine ([^{18}F]-FDA), [^{18}F]-fluorodihydroxyphenylalanine ([^{18}F]-FDOPA), [^{18}F]-fluoro-2-deoxy-D-glucose ([^{18}F]-FDG) PET/CT as well as CT/MRI.

Experimental Design: [^{68}Ga]-DOTATATE PET/CT was prospectively performed in 17 patients with *SDHB*-related metastatic PHEOs/PGLs. All patients also underwent [^{18}F]-FDG PET/CT and CT/MRI, with 16 of the 17 patients also receiving [^{18}F]-FDOPA and [^{18}F]-FDA PET/CT scans. Detection rates of metastatic lesions were compared between all these functional imaging studies. A composite synthesis of all used functional and anatomical imaging studies served as the imaging comparator.

Results: [^{68}Ga]-DOTATATE PET/CT demonstrated a lesion-based detection rate of 98.6% [95% confidence interval (CI), 96.5%–99.5%], [^{18}F]-FDG, [^{18}F]-FDOPA, [^{18}F]-FDA PET/CT, and CT/MRI showed detection rates of 85.8% (CI, 81.3%–89.4%; $P < 0.01$), 61.4% (CI, 55.6%–66.9%; $P < 0.01$), 51.9% (CI, 46.1%–57.7%; $P < 0.01$), and 84.8% (CI, 80.0%–88.5%; $P < 0.01$), respectively.

Conclusions: [^{68}Ga]-DOTATATE PET/CT showed a significantly superior detection rate to all other functional and anatomical imaging modalities and may represent the preferred future imaging modality in the evaluation of *SDHB*-related metastatic PHEO/PGL. *Clin Cancer Res; 21(17); 3888–95. ©2015 AACR.*

See related commentary by Hofman and Hicks, p. 3815

Introduction

Pheochromocytomas/paragangliomas (PHEO/PGL) are tumors derived from sympathetic tissue in adrenal or extra-adrenal abdominal locations or from parasympathetic tissue in the thorax or head and neck (1). More than 35% of PHEOs/PGLs are hereditary, including multiple endocrine neoplasia 2 (MEN2), von Hippel–Lindau syndrome (VHL), and neurofibromatosis 1 (NF1). In recent years, gene mutations encoding the four subunits of the succinate dehydrogenase (*SDH*) complex (2, 3), fumarate hydratase (*FH*; ref. 4), MYC-associated factor X (*MAX;* ref. 5), and hypoxia-inducible factor 2α (*HIF2A*; ref. 6) have been evaluated and often found to be associated with the presence of multiple and metastatic PHEOs/PGLs.

More than 40% of metastatic PHEOs/PGLs are related to succinate dehydrogenase subunit *B* (*SDHB*) mutation carriers (7), who are at high risk for developing metastatic disease. Some studies show a risk of up to 90% (8), with an only 36% 5-year probability of survival after diagnosis of metastatic disease (7). Proper staging and early detection of metastatic disease and evaluation of the extent of metastatic disease in these high risk patients is crucial and has a major effect on a patient's prognosis, including choosing the necessary treatment and follow-up (9).

Current treatment options in metastatic PHEOs/PGLs are limited and consist of radionuclide therapy with [^{131}I]-metaiodobenzylguanidine (MIBG) and chemotherapy with cyclophosphamide, vincristine, and dacarbazine (CVD; refs. 10, 11). Surgery and external beam radiotherapy are less commonly used options

[1]Program in Adult and Reproductive Endocrinology, *Eunice Kennedy Shriver* National Institute of Child Health and Human Development, NIH, Bethesda, Maryland. [2]Department of Radiology and Nuclear Medicine, Section of Nuclear Medicine, University Hospital Schleswig Holstein, Campus Lübeck, Lübeck, Germany. [3]Nuclear Medicine Department, Bichat Hospital, Paris, France. [4]Nuclear Medicine Division, Radiology and Imaging Sciences, NIH Clinical Center, Bethesda, Maryland. [5]Positron Emission Tomography Department, NIH Clinical Center, NIH, Bethesda, Maryland. [6]Department of Nuclear Medicine, La Timone University Hospital, CERIMED, Aix-Marseille University, Marseille, France. [7]Endocrine Oncology Branch, National Cancer Institute, Bethesda, Maryland. [8]Department of Internal Medicine I, University Hospital Schleswig Holstein, Campus Lübeck, Lübeck, Germany. [9]Center for Cancer Research, National Cancer Institute, Bethesda, Maryland.

Note: Supplementary data for this article are available at Clinical Cancer Research Online (http://clincancerres.aacrjournals.org/).

Corresponding Author: Karel Pacak, NIH, 10 Center Drive MSC-1109, Building 10, Room 1E-3140, Bethesda, MD 20892. Phone: 301-402-4592; Fax: 1-301-402-4712; E-mail: karel@mail.nih.gov

doi: 10.1158/1078-0432.CCR-14-2751

Published OnlineFirst April 14, 2015; DOI: 10.1158/1078-0432.CCR-14-2751

Translational Relevance

Patients with succinate dehydrogenase subunit *B* (*SDHB*) mutation–related pheochromocytoma/paraganglioma (PHEO/PGL) are known to suffer from aggressive tumor behavior that has a very high likelihood of metastasis. This work focuses solely on the performance of [^{68}Ga]-DOTA (0)-Tyr(3)-octreotate ([^{68}Ga]-DOTATATE) PET/CT in patients with metastatic *SDHB*-related PHEOs/PGLs and demonstrates the superiority of [^{68}Ga]-DOTATATE PET/CT in the detection of metastatic lesions in these patients, compared with all other and currently recommended functional imaging modalities. Our results may suggest modifying the functional imaging algorithm for these patients, dependent on the clinical setting, which currently places [^{18}F]-fluoro-2-deoxy-D-glucose ([^{18}F]-FDG) PET/CT as the gold standard. Furthermore, our results indicate that peptide receptor radionuclide therapy or treatment with so-called "cold" somatostatin receptor analogues, long-awaited remedies, could be used as new and promising therapeutic options for patients with metastatic *SDHB*-related PHEOs/PGLs.

in some patients. However, at least 50% of patients with metastatic PHEOs/PGLs, especially those with *SDHB* mutations, do not benefit from [^{131}I]-MIBG treatment due to a lack of the norepinephrine transporter system, resulting in suboptimal or no [^{131}I]-MIBG uptake (12). The use of CVD is a good alternative, but is reserved for patients with rapidly growing tumors or extensive organ tumor burden (especially in the liver) and limited by treatment-related toxicity. Thus, there is great interest and need to find new means of therapeutic options, including radionuclide therapy.

PHEOs/PGLs, similar to other neuroendocrine tumors (NET), are known to express somatostatin receptors (SSTR; ref. 13), and new, promising radiolabeled DOTA peptides for SSTR imaging and SSTR-targeting treatment have been developed.

Compared with [^{111}In]-DTPA-octreotide (Octreoscan), which is used for SSTR scintigraphy, the newly developed DOTA peptides, such as DOTA(0)-Tyr(3)-octreotate (DOTATATE), DOTA (0)-Phe(1)-Tyr(3)-octreotide (DOTATOC), and DOTA(1)-Nal (3)-octreotide (DOTANOC), bind to SSTR-expressing tumors much more effectively (14). In particular, DOTATATE has a very high affinity for SSTR2 (14), which is overexpressed in most PHEOs/PGLs (13), and has recently been used for their localization (15). Increased expression of SSTR2A and SSTR3 was recently shown in PHEOs/PGLs with *SDH* deficiency (16), including *SDHB* mutations.

DOTA peptides can be labeled with either the diagnostic positron emission tomography (PET) tracer [^{68}Ga] or therapeutic β-emitters such as [^{177}Lu] or [^{90}Y]. On the one hand, they can provide sensitive SSTR imaging, enabling improved anatomic localization using PET/computed tomography (CT) technique (17) compared with SSTR scintigraphy. On the other hand, when bound to therapeutic β-emitters, they can be, and are, used for peptide receptor radionuclide therapy (PRRT) in SSTR-overexpressing tumors, especially gastroenteropancreatic NETs (18). Treatment results in metastatic PHEOs/PGLs are also promising (19).

The present study had two main aims: first, to evaluate [^{68}Ga]-DOTATATE PET/CT in patients with metastatic *SDHB*-related PHEOs/PGLs and assess their eligibility for future PRRT as a new and needed therapeutic approach; and, second, to assess the diagnostic value of [^{68}Ga]-DOTATATE PET/CT in comparison with other well-established and currently recommended functional imaging studies in PHEOs/PGLs (20), including [^{18}F]-fluorodopamine ([^{18}F]-FDA), [^{18}F]-fluorodihydroxyphenylalanine ([^{18}F]-FDOPA), [^{18}F]-fluoro-2-deoxy-D-glucose ([^{18}F]-FDG) PET/CT, and in comparison with CT/MRI. Because histologic proof was not possible in many metastatic lesions, the composite of both anatomical and all functional imaging tests was considered the imaging comparator.

Patients and Methods

Patients

Between January and December 2014, 17 consecutive patients (11 men and 6 women) with *SDHB* mutation–associated PHEOs/PGLs with a mean age of 40.3 ± 14.0 years were prospectively evaluated at the *Eunice Kennedy Shriver* National Institute of Child Health and Human Development (NICHD) at the NIH. All patients had proven metastatic PHEOs/PGLs based on clinical evaluation, including previously found and surgically removed PHEOs/PGLs, biochemical diagnosis, and anatomical and functional imaging.

The study protocol was approved by the Institutional Review Board of the *Eunice Kennedy Shriver* NICHD (protocol: 00-CH-0093). All patients provided written informed consent for all clinical, genetic, biochemical, and imaging studies regarding PHEOs/PGLs.

Mean age at diagnosis of primary PHEO/PGL in these patients was 30.2 ± 15.0 years. The average interval between diagnosis of a primary tumor and referral to the NIH was 4.5 ± 3.8 years. All 17 patients previously underwent resection of their primary PHEO/PGL. Individual patient characteristics are summarized in Table 1.

Imaging techniques

CT scans of the neck, chest, abdomen, and pelvis were performed using the following devices: Siemens Somatom Definition AS, Siemens Somatom Definition Flash, Siemens Medical Solutions; Toshiba Aquilion ONE, Toshiba Medical Systems. Section thickness was up to 3 mm in the neck and 5 mm through the chest, abdomen, and pelvis. All studies were performed with intravenous (i.v.) rapid infusion of nonionic water-soluble contrast agent as well as oral contrast material.

MR scans of the neck, chest, abdomen, and pelvis were obtained with 1.5 and 3 Tesla scanners (Philips Achieva 1.5 and 3 Tesla, Philips Medical Systems; Siemens Verio 1.5 Tesla, Siemens Medical Solutions). Image thickness was 5 mm for all neck studies and 6 mm for chest, abdominal, and pelvic scans. Pre- and postinjection images were obtained in the axial plane. All MR scans included axial T2 series with and without fat saturation, STIR series, and T1 pre- and post-contrast series. MR scans of the abdomen and pelvis also included axial T1 in and out of phase and dynamic THRIVE during infusion of contrast, followed by delayed axial and coronal post-contrast scans after i.v. injection of a gadolinium-diethylenetriamine pentaacetic acid contrast agent.

All 17 patients underwent [^{68}Ga]-DOTATATE, [^{18}F]-FDG PET/CT scanning, and CT/MRI, with 16 also receiving [^{18}F]-FDOPA and [^{18}F]-FDA PET/CT scans.

Published OnlineFirst April 14, 2015; DOI: 10.1158/1078-0432.CCR-14-2751

Table 1. Individual patient characteristics

Pt. #	Sex	*SDHB* mutation	Age (d)	Age (s)	LOP	Hyper secretion	TTM	LOM	Treatment
1	m	c.725G>A, p.Arg242His	20	34	R skull	None	12	B	RT skull
2	f	c.688C>T, p.Arg230Cys	22	25	L carotid body	None	0	B, Lu, Me	Res primary
3	m	c.418G>T, p.Val140Phe	10	20	Aortic bifurcation	NE, NMN, DA	0	B, A/P	Res primary
4	m	c.689G>A, p.Arg230His	52	52	R para-adrenal	NE, NMN	0	B	RT skull Res primary
5	f	c.343C>T, p.Arg115X	32	43	Urinary bladder	NE, NMN	3	B, Lu, A/P	Res primary, CVD
6	f	c.689G>A, p.Arg230His	28	50	L carotid body	None	20	Lu, Li	Res primary, CVD
7	f	c.136C>T, p.Arg46X	19	24	R glomus jugulare	None	0	B, Ne	Res primary, RT skull
8	m	c.200+33G>A, p.Glu228Glyfsx27	47	59	L para-adrenal	DA, MTT	3	Me, Ne, A/P	Res. primary
9	m	c.136C>T, p.Arg46X	45	46	urinary bladder	NE, NMN,	0	Lu, B	Res primary
10	m	c.136C>T, p.Arg46X	25	37	R mediastinal	None	0	Lu	Res primary, CVD
11	m	c.72+1G>T	54	60	R para-adrenal	NE, NMN	0	Lu, Me, A/P, B	Res primary, MIBG
12	f	Exon 1 deletion	49	55	Aortic bifurcation	NE, NMN, DA, MTT	0	Ne, Me, A/P	Res primary, MIBG
13	m	c.330_331del, p.Leu111SerfsX7	10	23	L adrenal	NE, NMN	0	B, Lu, Ne, A/P, Li	Res primary
14	m	c.268C>T, p.Arg90X	11	26	R adrenal	None	8	B, Lu, Ne	Res primary, MIBG
15	m	Exon 1 deletion	34	41	R para-adrenal	NMN, DA, MTT	5	Me, B	Res primary
16	m	c.137G>A, p.Arg46Gln	19	36	L pelvis	NE, NMN, DA, MTT	13	B, Lu, Ne, A/P	Res primary, MIBG, CVD
17	f	c.541-2A>G, splice site mutation	36	54	L carotid body	NE, NMN, DA, MTT	8	B	Res primary

Abbreviations: Age (d), age at diagnosis; age (s), age at study; A/P, abdomen/pelvis; B, bones; CVD, chemotherapy with CVD; DA, dopamine; f, female, L, left; LOM, location of metastases; LOP, location of primary; Lu, lungs; m, male; Me, mediastinum, MIBG, ^{131}I-MIBG treatment; Mtt, methoxytyramine; Ne, neck; NE, norepinephrine; NMN, normetanephrine; no, number; Pat., patient; R, right; Res, surgical resection; RT, radiotherapy; TTM, time to metastases (years).

PET/CT scans from the upper thighs to the skull were performed 60 minutes after i.v. injection of a mean administered activity of 201.8 ± 39.6 MBq [^{68}Ga]-DOTATATE, 60 minutes after 362.8 ± 112 MBq [^{18}F]-FDG, 30 minutes after 458.5 ± 83.1 MBq [^{18}F]-FDOPA, and approximately 8 minutes after 37.2 ± 1.1 MBq [^{18}F]-FDA. Sixty minutes before each [^{18}F]-FDOPA scan, 200 mg of carbidopa was administered orally. All PET/CT scans were performed on a Siemens Biograph-mCT 128 PET/CT scanner (Siemens Medical Solutions). PET imaging was obtained in three-dimensional mode. PET images were reconstructed on a 256 × 256 matrix using an iterative algorithm provided by the manufacturer, which also uses time of flight. Low-dose CT studies for attenuation correction and anatomic coregistration were performed without contrast and used for anatomical localization only.

Analysis of data

[^{68}Ga]-DOTATATE PET/CT studies were each read independently by two nuclear medicine physicians blinded to all imaging and clinical data except for the diagnosis, sex, and age of the patient.

Maximal standardized uptake values (SUV_{max}) were determined, and focal areas of abnormal uptake showing a higher SUV_{max} than surrounding tissue were considered as lesions. Discrepancies, which occurred in 6 lesions with a mean SUV of 6.2 ± 5.6 in 4 patients, were solved by consensus review. In all other imaging studies, physicians were blinded to [^{68}Ga]-DOTATATE PET/CT scans and clinical data, except for diagnosis, sex, age of the patient, and previous imaging studies. All imaging studies were performed within 22 ± 15 days of each other. For regional analysis, adrenal glands, liver, abdominal/pelvic compartments (excluding adrenal glands and liver), lungs, mediastinum, and bone were analyzed separately. A patient or region was considered positive regardless of the number of positive findings. Patient-to-patient, region-to-region, and lesion-to-lesion analyses were performed. If the number of lesions in a region exceeded 15, the count was truncated at 15. Patient-, region-, and lesion-related detection rates were compared. Head and neck PGLs were excluded from the analysis in patients with head and neck PGLs and sympathetic PGLs.

Histologic proof of metastatic lesions was not feasible. The composite of anatomic and all performed functional imaging tests was considered the imaging comparator. A positive result on at least two different functional imaging modalities or at least one functional imaging study and CT/MRI was counted as true disease, whereas a lesion detected only on CT/MRI or only on one functional imaging test, while negative on all other used imaging tests, was considered a false-positive imaging result.

Statistical analysis

Results are given as means with 95% confidence intervals (CI) unless stated otherwise. For statistical analysis, the McNemar test was used to compare sensitivities between [^{68}Ga]-DOTATATE PET/CT and the other imaging modalities. A two-sided $P < 0.05$ was considered significant.

Results

[^{68}Ga]-DOTATATE PET/CT had a lesion-based detection rate of 98.6% (CI, 96.5%–99.5%), identifying 285 of 289 lesions (mean SUV 56.0 ± 62.1) compared with our defined imaging comparator. Significantly more lesions were identified on [^{68}Ga]-DOTATATE PET/CT than on all other used functional imaging modalities and CT/MRI (two-sided $P < 0.01$ for each imaging modality compared with [^{68}Ga]-DOTATATE PET/CT; corresponding cross tables in Supplementary Fig. S1). Lesion-based findings on [^{68}Ga]-DOTATATE PET/CT compared with all other used functional imaging modalities and CT/MRI are summarized and outlined in Tables 2 and 3 as well as in Fig. 1. Metastatic lesions were found in the mediastinum, lungs, liver, abdomen/pelvis, and bones. Those in the mediastinum, abdomen, or pelvis were located in lymphatic nodes. Three bone lesions, which were positive on [^{18}F]-FDA and [^{18}F]-FDG PET/CT, and one lung lesion, which was positive on [^{18}F]-FDG PET/CT and anatomical imaging, were not identified by [^{68}Ga]-DOTATATE PET/CT. A lesion-based evaluation excluding the patient who only received [^{68}Ga]-DOTATATE, [^{18}F]-FDG PET/CT, and CT/MRI did not lead to any statistical change.

Besides the 285 lesions confirmed by the defined imaging comparator, [^{68}Ga]-DOTATATE PET/CT detected 33 additional

Published OnlineFirst April 14, 2015; DOI: 10.1158/1078-0432.CCR-14-2751

Table 2. Number of identified lesions in [^{68}Ga]-DOTATATE, [^{18}F]-FDA-, [^{18}F]-FDOPA-, [^{18}F]-FDG-PET/CT, and CT/MRI compared with lesions identified by the imaging comparator

Lesions	[^{68}Ga]-DOTATATE	[^{18}F]-FDG	[^{18}F]-FDOPA	[^{18}F]-FDA	CT/MRI
All compartments	285/289	248/289	175/285	148/285	245/289
Mediastinum	65/65	57/65	39/65	39/65	55/65
Lungs	62/63	45/63	45/63	18/63	62/63
Abdomen	43/43	40/43	31/43	19/43	33/43
Liver	5/5	3/5	4/5	0/5	5/5
Bone	95/98	91/98	41/94	57/94	82/98

lesions: 8 in mediastinal lymphatic nodes, 10 in retroperitoneal and pelvic lymphatic nodes, and 15 bone lesions (mean SUV 8.2 ± 6.4). All lesions were in the field of view of CT/MR. In the anatomical imaging studies CT/MRI, 8 lesions were reported, which were not positive on any functional imaging study. Two were retroperitoneal lymphatic nodes (1.5 cm and 1.6 cm), 4 were in the lungs (0.4–0.8 cm), and two in the liver (0.7 cm and 0.8 cm). Three mediastinal lesions were only positive in [^{18}F]-FDG PET/CT. Not a single lesion was only positive in either [^{18}F]-FDOPA or [^{18}F]-FDA PET/CT but not another functional or anatomic imaging test.

Per patient detection rates of [^{68}Ga]-DOTATATE, [^{18}F]-FDG, [^{18}F]-FDOPA, [^{18}F]-FDA PET/CT, and CT/MRI were 100% (17 of 17 patients), CI, 81.6%–100%, 100% (17/17); CI, 81.6%–100%, 87.5% (14/16); CI, 64.0%–96.5%, 81.3% (13/16); CI, 57.0%–93.4%, and 100% (17/17), CI, 81.6%–100%, respectively.

The per region detection rate for [^{68}Ga]-DOTATATE was 100%, identifying 42 of 42 regions (42/42); CI, 91.6%–100%, 97.6% for [^{18}F]-FDG (41/42); CI, 87.7%–99.6%, 65.9% for [^{18}F]-FDOPA (27/41); CI, 50.6%–78.4%, 58.4% for [^{18}F]-FDA PET/CT (24/41); CI, 43.4%–72.2%, and 95.2% for CT/MRI (40/42), CI, 84.2%–98.7%.

A PET-imaging example comparing [^{68}Ga]-DOTATATE, [^{18}F]-FDG, [^{18}F]-FDOPA, and [^{18}F]-FDA PET/CT is shown in Fig. 2.

Discussion

In this study, we evaluated [^{68}Ga]-DOTATATE PET/CT in a cohort of patients with *SDHB*-related metastatic PHEOs/PGLs in comparison with [^{18}F]-FDA, [^{18}F]-FDOPA, [^{18}F]-FDG PET/CT, and CT/MRI. The composite of both anatomical and all functional imaging tests was considered the imaging comparator.

[^{68}Ga]-DOTATATE PET/CT demonstrated a lesion-based detection rate of 98.6% (CI, 96.5%–99.5%), which was significantly superior to all other imaging modalities in this study, thus demonstrating the utility of this modality in localizing tumors in *SDHB*-related PHEO/PGL. We feel that this modality will also be useful in determining the possible eligibility for PRRT in patients with *SDHB*-related PHEO/PGL.

Functional imaging agents are able to target PHEOs/PGLs through different mechanisms. [^{18}F]-FDA and [^{123}I]-MIBG specifically target catecholamine synthesis, storage, and secretion pathways, and both enter the cell via the norepinephrine transporter (21, 22). In this study, [^{18}F]-FDA had a low lesion-based detection rate of 51.9% (CI, 46.1%–57.7%), which might be explained by tumor dedifferentiation associated with loss of the norepinephrine transporter in these patients. This is supported by the reported [^{123}I]-MIBG negativity of more than 50% of patients in *SDHB* mutation–associated PHEOs/PGLs (12). Six of the patients in our study had undergone [^{123}I]-MIBG scintigraphy with a very low lesion detection rate of 18.7% (CI, 12.0%–27.9%), but this result was most likely biased by the small patient cohort and the heavy disease burden of our patient population.

[^{18}F]-FDOPA targets cells via the amino acid transporter system (23) and has demonstrated excellent results in patients with *SDHx* mutation–related head and neck PGLs (24). However, the lesion-based sensitivity of [^{18}F]-FDOPA in *SDHB*-related PHEOs/PGLs outside the head and neck regions has been shown to be poor in a previous study (25). The detection rate in our study reached 61.4% (CI, 55.6%–66.9%).

[^{18}F]-FDG is a sensitive but nonspecific radiopharmaceutical that enters the cell via glucose transporters (GLUT; ref. 26). Its accumulation is related to increased glucose metabolism as seen in many different types of tumors (26). In *SDHB*-related metastatic PGLs, its high sensitivity has been well documented (27–29). Higher SUVs compared with sporadic and other hereditary PHEO/PGL are also reported, accompanied by an upregulation of hexokinases 2 and 3 (30). Further, it is known that a mutation in the succinate dehydrogenase complex II subunit B can lead to a downregulation or loss of succinate dehydrogenase enzyme activity in the Krebs cycle, resulting in an upregulation of hypoxic angiogenetic pathways via HIFs (6), which force tumor cells to shift from oxidative phosphorylation to aerobic glycolysis (Warburg effect; ref. 31). Currently, [^{18}F]-FDG PET/CT is recommended as the functional imaging technique of choice for patients with metastatic PHEOs/PGLs, including their follow-up and assessment of treatment-related responses (20, 32). In this study, we found a lesion-based detection rate of 85.8% (CI, 81.3%–89.4%) for [^{18}F]-FDG PET/CT.

With a lesion-based detection rate of 98.6% (CI, 96.5%–99.5%), [^{68}Ga]-DOTATATE PET/CT was significantly superior to all other functional imaging modalities in this study. [^{68}Ga]-

Table 3. Detection rate (%) and 95% CI (%) for [^{68}Ga]-DOTATATE, [^{18}F]-FDA-, [^{18}F]-FDOPA-, [^{18}F]-FDG-PET/CT, and CT/MRI

Detection rate	[^{68}Ga]-DOTATATE	[^{18}F]-FDG	[^{18}F]-FDOPA	[^{18}F]-FDA	CT/MRI
All compartments	98.6 (96.5–99.5)	85.8 (81.3–89.4)	61.4 (55.6–66.9)	51.9 (46.1–57.7)	84.8 (80.0–88.5)
Mediastinum	100 (94.4–100)	87.7 (77.6–93.6)	60.0 (47.9–71.0)	60.0 (47.9–71.0)	84.6 (73.9–91.4)
Lungs	98.4 (92.5–99.7)	71.4 (59.3–81.1)	71.4 (59.3–81.1)	28.6 (18.9–40.7)	98.4 (91.5–99.7)
Abdomen	100 (91.8–100)	93.0 (81.4–97.6)	72.1 (57.3–83.3)	44.2 (30.4–58.9)	76.7 (62.3–88.7)
Liver	100 (56.5–100)	60.0 (23.1–88.2)	80.0 (37.6–96.4)	0% (0.0–43.5)	100 (56.5–100)
Bone	96.9 (91.4–99.0)	92.9 (86.0–96.5)	43.6 (34.0–53.7)	60.6 (50.5–69.9)	83.7 (75.1–89.7)

Published OnlineFirst April 14, 2015; DOI: 10.1158/1078-0432.CCR-14-2751

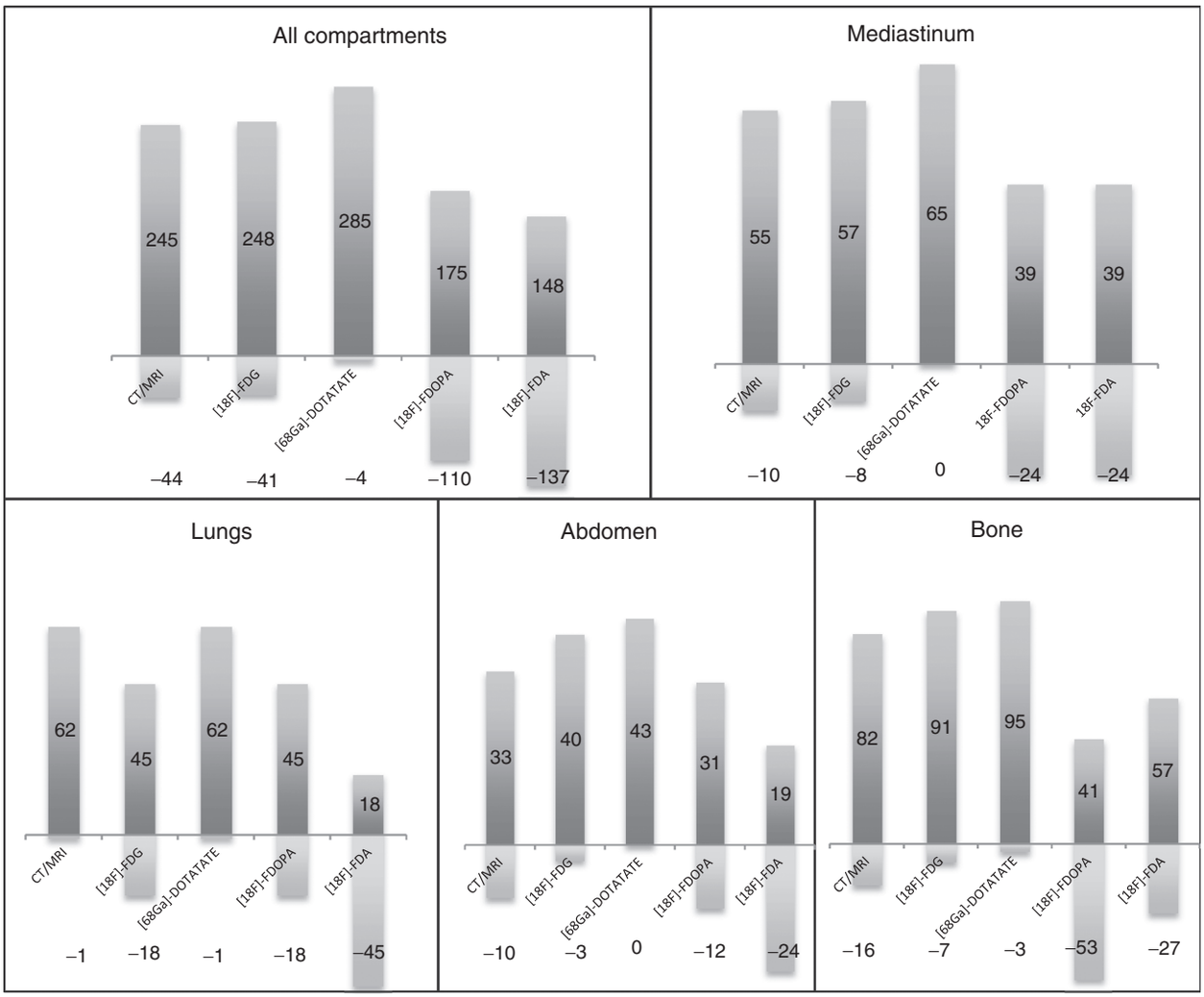

Figure 1.
Identified lesions (positive columns) and missed lesions (negative columns) for CT/MRI, [^{18}F]-FDG, [^{68}Ga]-DOTATATE, [^{18}F]-FDOPA, and [^{18}F]-FDA PET/CT.

DOTATATE, which is known to have an approximately 10-fold higher affinity for SSTR2 than [^{68}Ga]-DOTATOC (which also has high affinity to SSTR5) and an approximately 100-fold higher affinity for SSTR2 than [^{111}In]-DTPA-octreotide (14), has already shown excellent results in the imaging of SSTR2-expressing gastroenteropancreatic NETs (33), and PHEOs/PGLs are also known to overexpress predominantly SSTR2 (13). A recent study has also demonstrated an increased expression of SSTR2A and SSTR3 in PHEOs/PGLs with *SDH* deficiency (16), which also supports the approach of SSTR imaging and treatment in these tumors. Until now, there have only been a few small and heterogeneous studies and case reports on imaging of PHEOs/PGLs with DOTA analogues. These have shown high sensitivities of [^{68}Ga]-DOTATATE and [^{68}Ga]-DOTATOC PET/CT, approaching or reaching 100% (17, 34).

Besides its diagnostic value, [^{68}Ga]-DOTATATE PET/CT can be used to determine which patients may benefit from PRRT, which would be a desirable new treatment option for these patients (7, 8). Although PRRT has not been specifically evaluated in *SDHB*-related PHEOs/PGLs yet, it has already been shown to lead to longer progression-free survival, mainly in gastroenteropancreatic NETs (18), but also in other metastatic NETs, including PHEOs/PGLs (35). Unfortunately, PRRT is not approved by the FDA at present. In the meanwhile, the high sensitivity of [^{68}Ga]-DOTATATE PET/CT in *SDHB*-related metastatic PHEO/PGL suggests that these patients can be treated with cold SSTR analogues, including sandostatin LAR, lanreotide, or others. Although this approach has not yet been evaluated in PHEOs/PGLs, results using lanreotide in gastroenteropancreatic NETs (36) and individual reports of octreotide treatment in patients with head and neck PGLs support this approach (37, 38). This could also be extremely useful for patients in whom the location or extension of a PHEO/PGL lesion (especially skull base) cannot be accessed by any surgical approach.

The phenomenon of additional lesions appearing with [^{68}Ga]-DOTA analogues PET/CT that were not seen by other imaging studies has been reported before (15, 17). Because histologic proof of these lesions in our study was not possible, these lesions

Published OnlineFirst April 14, 2015; DOI: 10.1158/1078-0432.CCR-14-2751

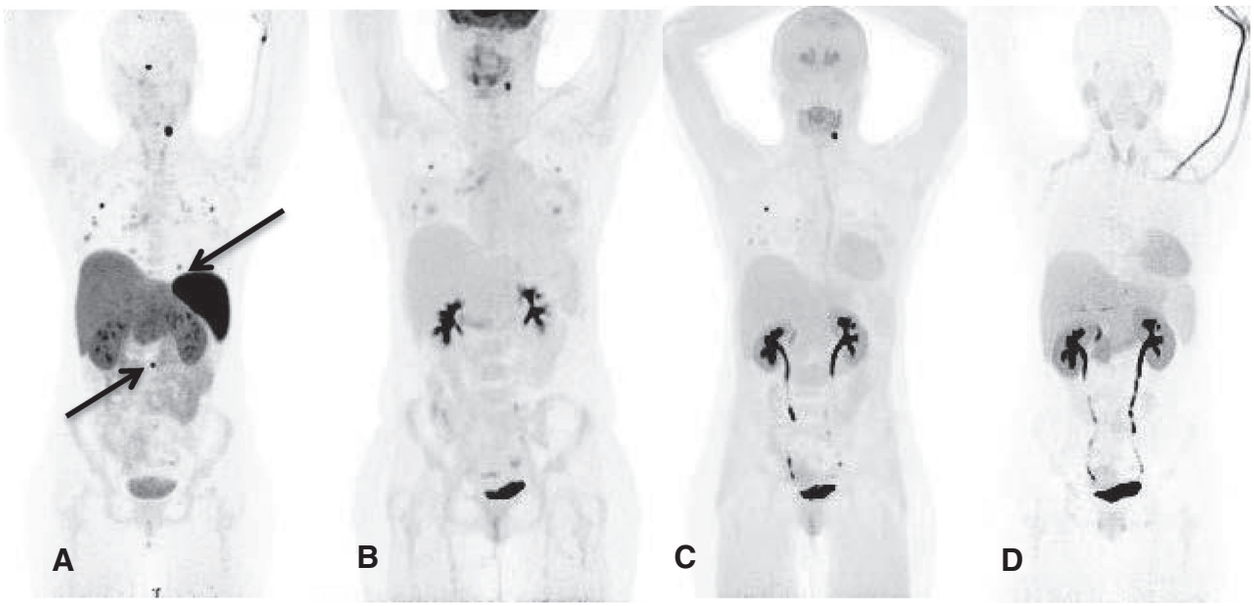

Figure 2.
Twenty-four-year-old female patient with metastatic paraganglioma and *SDHB* mutation, first diagnosed with left carotid body tumor, lung and bone metastases in 2011. [^{68}Ga]-DOTATATE PET (A) demonstrated additional lung and bone lesions (arrows), compared with [^{18}F]-FDG PET (B) and [^{18}F]-FDOPA PET (C). [^{18}F]-FDA PET (D) and [^{123}I]-MIBG scintigraphy (not shown) were negative.

have to be discussed as false-positive lesions. On the other hand, studies have also reported histologic confirmation of SSTR-positive tumor tissue in such cases, which led to a treatment change in up to 60% of patients (39).

Finally, the high detection rate of [^{68}Ga]-DOTATATE PET/CT in these patients also suggests that the high malignant potential and presumed dedifferentiation of metastatic PHEOs/PGLs in *SDHB* mutations apparently do not lead to a significant loss of SSTR expression. This is supported by the increased SSTR2A and SSTR3 expression, which was found in *SDH*-deficient tumors (16). Recently, SSTR expression with positive [^{68}Ga]-DOTATOC PET/CT was also shown in patients with undifferentiated Epstein–Barr virus–related nasopharyngeal cancer (40). This also indicates that a loss in tumor differentiation is not necessarily combined with a loss in SSTR expression.

In the current guidelines, which do not yet take PET imaging with [^{68}Ga]-DOTA peptides into consideration, [^{18}F]-FDG is recommended as first-line functional imaging of *SDHB*-related PHEO/PGL (20). However, our results indicate that [^{68}Ga]-DOTATATE PET/CT may have an incremental diagnostic value in the detection of disease sites, which could have an impact on patient care. Therefore, we believe that future guidelines may modify the recommendations in favor of using [^{68}Ga]-DOTA peptides, especially if confirming results from a larger number of patients, sporadic PHEO/PGL patients, and other PHEO/PGL genotypes are made available.

In clinical settings, such as the evaluation of treatment response after systemic radionuclide therapy or chemotherapy, the use of [^{68}Ga]-DOTATATE PET/CT is still unclear and has to be evaluated. In clinical settings of doubtful CT/MRI results, [^{68}Ga]-DOTATATE might also be helpful, although potential false-positive results could occur. The more specific functional imaging studies such as [^{18}F]-FDOPA and [^{18}F]-FDA PET/CT seem to harbor a higher risk for false-negative results. Finally, [^{18}F]-FDOPA PET/CT and especially [^{18}F]-FDA PET/CT are of limited availability, whereas for [^{68}Ga]-DOTATATE PET/CT, we believe that broader clinical availability can be expected in the future.

Our study was subject to certain limitations, including the relatively small number of patients and possible bias related to our chosen reference test. Based on this imaging comparator, combined positive findings in functional and/or anatomical imaging studies, on the one hand, cannot fully exclude false-positive results (e.g., possible positive lesions in [^{68}Ga]-DOTATATE PET/CT, [^{18}F]-FDG-PET/CT, and/or CT/MRI related to inflammation or possible positive lesions in [^{68}Ga]-DOTATATE PET/CT, [^{18}F]-FDOPA PET/CT, and/or CT/MRI related to different NETs). On the other hand, true-positive findings, which only appear in one imaging modality, e.g., CT/MRI, would have been counted as false positive in our setting.

In conclusion, although [^{18}F]-FDG PET/CT is currently recommended as the functional imaging technique of choice in *SDHB*-related PHEOs/PGLs, and our study is subject to certain limitations, we believe that our results may indicate a preference for [^{68}Ga]-DOTATATE PET/CT in these patients, particularly in the detection of progressive metastatic disease, additional disease sites, and even early detection of metastatic disease. [^{68}Ga]-DOTATATE PET/CT can also be used to help determine the eligibility of patients for PRRT, a new and hopefully soon to be available treatment option. The utility of [^{68}Ga]-DOTATATE PET/CT in other genotypes, sporadic PHEO/PGL, or for treatment monitoring should be evaluated soon.

Disclosure of Potential Conflicts of Interest

No potential conflicts of interest were disclosed.

Published OnlineFirst April 14, 2015; DOI: 10.1158/1078-0432.CCR-14-2751

Authors' Contributions

Conception and design: I. Janssen, E.M. Blanchet, C.M. Millo, H. Lehnert, K. Pacak

Development of methodology: E.M. Blanchet, C.M. Millo, P. Herscovitch, K. Pacak

Acquisition of data (provided animals, acquired and managed patients, provided facilities, etc.): I. Janssen, K. Adams, C.C. Chen, P. Herscovitch, E. Kebebew, A.T. Fojo, K. Pacak

Analysis and interpretation of data (e.g., statistical analysis, biostatistics, computational analysis): I. Janssen, C.M. Millo, D. Taieb, E. Kebebew, H. Lehnert, A.T. Fojo, K. Pacak

Writing, review, and/or revision of the manuscript: I. Janssen, E.M. Blanchet, C.C. Chen, C.M. Millo, P. Herscovitch, D. Taieb, E. Kebebew, H. Lehnert, K. Pacak

Administrative, technical, or material support (i.e., reporting or organizing data, constructing databases): C.C. Chen, K. Pacak

Study supervision: C.M. Millo, K. Pacak

Acknowledgments

The authors acknowledge the technical assistance of Joan Nambuba and Robert A. Wesley in the production of this article.

Grant Support

This work was supported, in part, by the Intramural Research Program of the NIH, *Eunice Kennedy Shriver* National Institute of Child Health and Human Development.

The costs of publication of this article were defrayed in part by the payment of page charges. This article must therefore be hereby marked *advertisement* in accordance with 18 U.S.C. Section 1734 solely to indicate this fact.

Received October 27, 2014; revised March 6, 2015; accepted March 23, 2015; published OnlineFirst April 14, 2015.

References

1. DeLellis RA. Pathology and genetics of tumours of endocrine organs. Lyon, France: IARC Press; 2004.
2. Timmers HJ, Kozupa A, Eisenhofer G, Raygada M, Adams KT, Solis D, et al. Clinical presentations, biochemical phenotypes, and genotype-phenotype correlations in patients with succinate dehydrogenase subunit B-associated pheochromocytomas and paragangliomas. J Clin Endocrinol Metab 2007;92:779–86.
3. Brouwers FM, Eisenhofer G, Tao JJ, Kant JA, Adams KT, Linehan WM, et al. High frequency of SDHB germline mutations in patients with malignant catecholamine-producing paragangliomas: implications for genetic testing. J Clin Endocrinol Metab 2006;91:4505–9.
4. Castro-Vega LJ, Buffet A, De Cubas AA, Cascon A, Menara M, Khalifa E, et al. Germline mutations in FH confer predisposition to malignant pheochromocytomas and paragangliomas. Hum Mol Genet 2014;23:2440–6.
5. Burnichon N, Cascon A, Schiavi F, Morales NP, Comino-Mendez I, Abermil N, et al. MAX mutations cause hereditary and sporadic pheochromocytoma and paraganglioma. Clin Cancer Res 2012;18:2828–37.
6. Jochmanova I, Yang C, Zhuang Z, Pacak K. Hypoxia-inducible factor signaling in pheochromocytoma: turning the rudder in the right direction. J Natl Cancer Inst 2013;105:1270–83.
7. Amar L, Baudin E, Burnichon N, Peyrard S, Silvera S, Bertherat J, et al. Succinate dehydrogenase B gene mutations predict survival in patients with malignant pheochromocytomas or paragangliomas. J Clin Endocrinol Metab 2007;92:3822–8.
8. Matro J, Giubellino A, Pacak K. Current and future therapeutic approaches for metastatic pheochromocytoma and paraganglioma: focus on SDHB tumors. Horm Metab Res 2013;45:147–53.
9. Taieb D, Neumann H, Rubello D, Al-Nahhas A, Guillet B, Hindie E. Modern nuclear imaging for paragangliomas: beyond SPECT. J Nucl Med 2012;53:264–74.
10. van Hulsteijn LT, Niemeijer ND, Dekkers OM, Corssmit EP. (131)I-MIBG therapy for malignant paraganglioma and phaeochromocytoma: systematic review and meta-analysis. Clin Endocrinol 2014;80:487–501.
11. Huang H, Abraham J, Hung E, Averbuch S, Merino M, Steinberg SM, et al. Treatment of malignant pheochromocytoma/paraganglioma with cyclophosphamide, vincristine, and dacarbazine: recommendation from a 22-year follow-up of 18 patients. Cancer 2008;113:2020–8.
12. Fonte JS, Robles JF, Chen CC, Reynolds J, Whatley M, Ling A, et al. False-negative (1)(2)(3)I-MIBG SPECT is most commonly found in SDHB-related pheochromocytoma or paraganglioma with high frequency to develop metastatic disease. Endocr Relat Cancer 2012;19:83–93.
13. Reubi JC, Waser B, Schaer JC, Laissue JA. Somatostatin receptor sst1-sst5 expression in normal and neoplastic human tissues using receptor autoradiography with subtype-selective ligands. Eur J Nucl Med 2001;28:836–46.
14. Reubi JC, Schar JC, Waser B, Wenger S, Heppeler A, Schmitt JS, et al. Affinity profiles for human somatostatin receptor subtypes SST1-SST5 of somatostatin radiotracers selected for scintigraphic and radiotherapeutic use. Eur J Nucl Med 2000;27:273–82.
15. Maurice JB, Troke R, Win Z, Ramachandran R, Al-Nahhas A, Naji M, et al. A comparison of the performance of (6)(8)Ga-DOTATATE PET/CT and (1)(2)(3)I-MIBG SPECT in the diagnosis and follow-up of phaeochromocytoma and paraganglioma. Eur J Nucl Med Mol Imaging 2012;39:1266–70.
16. Elston MS, Meyer-Rochow GY, Conaglen HM, Clarkson A, Clifton-Bligh RJ, Conaglen JV, et al. Increased SSTR2A and SSTR3 expression in succinate dehydrogenase-deficient pheochromocytomas and paragangliomas. Hum Pathol 2015;46:390–6.
17. Hofman MS, Kong G, Neels OC, Eu P, Hong E, Hicks RJ. High management impact of Ga-68 DOTATATE (GaTate) PET/CT for imaging neuroendocrine and other somatostatin expressing tumours. J Med Imaging Radiat Oncol 2012;56:40–7.
18. Kwekkeboom DJ, de Herder WW, Kam BL, van Eijck CH, van Essen M, Kooij PP, et al. Treatment with the radiolabeled somatostatin analog [177 Lu-DOTA 0,Tyr3]octreotate: toxicity, efficacy, and survival. J Clin Oncol 2008;26:2124–30.
19. Zovato S, Kumanova A, Dematte S, Sansovini M, Bodei L, Di Sarra D, et al. Peptide receptor radionuclide therapy (PRRT) with 177Lu-DOTATATE in individuals with neck or mediastinal paraganglioma (PGL). Horm Metab Res 2012;44:411–4.
20. Lenders JW, Duh QY, Eisenhofer G, Gimenez-Roqueplo AP, Grebe SK, Murad MH, et al. Pheochromocytoma and paraganglioma: an endocrine society clinical practice guideline. J Clin Endocrinol Metab 2014;99:1915–42.
21. Sisson JC, Wieland DM. Radiolabeled meta-iodobenzylguanidine: pharmacology and clinical studies. Am J Physiol Imaging 1986;1:96–103.
22. Timmers HJ, Eisenhofer G, Carrasquillo JA, Chen CC, Whatley M, Ling A, et al. Use of 6-[18F]-fluorodopamine positron emission tomography (PET) as first-line investigation for the diagnosis and localization of non-metastatic and metastatic phaeochromocytoma (PHEO). Clin Endocrinol 2009;71:11–7.
23. Havekes B, King K, Lai EW, Romijn JA, Corssmit EP, Pacak K. New imaging approaches to phaeochromocytomas and paragangliomas. Clin Endocrinol 2010;72:137–45.
24. King KS, Chen CC, Alexopoulos DK, Whatley MA, Reynolds JC, Patronas N, et al. Functional imaging of SDHx-related head and neck paragangliomas: comparison of 18F-fluorodihydroxyphenylalanine, 18F-fluorodopamine, 18F-fluoro-2-deoxy-D-glucose PET, 123I-metaiodobenzylguanidine scintigraphy, and 111In-pentetreotide scintigraphy. J Clin Endocrinol Metab 2011;96:2779–85.
25. Timmers HJ, Chen CC, Carrasquillo JA, Whatley M, Ling A, Havekes B, et al. Comparison of 18F-fluoro-L-DOPA, 18F-fluoro-deoxyglucose, and 18F-fluorodopamine PET and 123I-MIBG scintigraphy in the localization of pheochromocytoma and paraganglioma. J Clin Endocrinol Metab 2009;94:4757–67.
26. Belhocine T, Spaepen K, Dusart M, Castaigne C, Muylle K, Bourgeois P, et al. 18FDG PET in oncology: the best and the worst. Int J Oncol 2006;28:1249–61.
27. Timmers HJ, Kozupa A, Chen CC, Carrasquillo JA, Ling A, Eisenhofer G, et al. Superiority of fluorodeoxyglucose positron emission tomography to

other functional imaging techniques in the evaluation of metastatic SDHB-associated pheochromocytoma and paraganglioma. J Clin Oncol 2007;25:2262–9.
28. Timmers HJ, Chen CC, Carrasquillo JA, Whatley M, Ling A, Eisenhofer G, et al. Staging and functional characterization of pheochromocytoma and paraganglioma by 18F-fluorodeoxyglucose (18F-FDG) positron emission tomography. J Natl Cancer Inst 2012;104:700–8.
29. Mann GN, Link JM, Pham P, Pickett CA, Byrd DR, Kinahan PE, et al. [11C]metahydroxyephedrine and [18F]fluorodeoxyglucose positron emission tomography improve clinical decision making in suspected pheochromocytoma. Ann Surg Oncol 2006;13:187–97.
30. van Berkel A, Rao JU, Kusters B, Demir T, Visser E, Mensenkamp AR, et al. Correlation between in vivo 18F-FDG PET and immunohistochemical markers of glucose uptake and metabolism in pheochromocytoma and paraganglioma. J Nucl Med 2014;55:1253–9.
31. Warburg O. On the origin of cancer cells. Science 1956;123:309–14.
32. Taieb D, Timmers HJ, Hindie E, Guillet BA, Neumann HP, Walz MK, et al. EANM 2012 guidelines for radionuclide imaging of phaeochromocytoma and paraganglioma. Eur J Nucl Med Mol Imaging 2012;39:1977–95.
33. Haug AR, Cindea-Drimus R, Auernhammer CJ, Reincke M, Wangler B, Uebleis C, et al. The role of 68Ga-DOTATATE PET/CT in suspected neuroendocrine tumors. J Nucl Med 2012;53:1686–92.
34. Kroiss A, Putzer D, Frech A, Decristoforo C, Uprimny C, Gasser RW, et al. A retrospective comparison between 68Ga-DOTA-TOC PET/CT and 18F-DOPA PET/CT in patients with extra-adrenal paraganglioma. Eur J Nucl Med Mol Imaging 2013;40:1800–8.
35. Imhof A, Brunner P, Marincek N, Briel M, Schindler C, Rasch H, et al. Response, survival, and long-term toxicity after therapy with the radiolabeled somatostatin analogue [90Y-DOTA]-TOC in metastasized neuroendocrine cancers. J Clin Oncol 2011;29:2416–23.
36. Caplin ME, Pavel M, Cwikla JB, Phan AT, Raderer M, Sedlackova E, et al. Lanreotide in metastatic enteropancreatic neuroendocrine tumors. N Engl J Med 2014;371:224–33.
37. Elshafie O, Al Badaai Y, Alwahaibi K, Qureshi A, Hussein S, Al Azzri F, et al. Catecholamine-secreting carotid body paraganglioma: successful preoperative control of hypertension and clinical symptoms using high-dose long-acting octreotide. Endocrinol Diabetes Metab Case Rep 2014;2014:140051.
38. Kau R, Arnold W. Somatostatin receptor scintigraphy and therapy of neuroendocrine (APUD) tumors of the head and neck. Acta Otolaryngol 1996;116:345–9.
39. Frilling A, Sotiropoulos GC, Radtke A, Malago M, Bockisch A, Kuehl H, et al. The impact of 68Ga-DOTATOC positron emission tomography/computed tomography on the multimodal management of patients with neuroendocrine tumors. Ann Surg 2010;252:850–6.
40. Schartinger VH, Dudas J, Url C, Reinold S, Virgolini IJ, Kroiss A, et al. (68)Ga-DOTA (0)-Tyr (3)-octreotide positron emission tomography in nasopharyngeal carcinoma. Eur J Nucl Med Mol Imaging 2015;42:20–4.

Published OnlineFirst April 14, 2015; DOI: 10.1158/1078-0432.CCR-14-2751

Clinical Cancer Research

Superiority of [^{68}Ga]-DOTATATE PET/CT to Other Functional Imaging Modalities in the Localization of *SDHB*-Associated Metastatic Pheochromocytoma and Paraganglioma

Ingo Janssen, Elise M. Blanchet, Karen Adams, et al.

Clin Cancer Res 2015;21:3888-3895. Published OnlineFirst April 14, 2015.